

Electronic Supplementary Information for:

**Glucosylthioureidocalix[4]arenes: synthesis, conformations and gas-phase recognition of amino acids**

Mika Torvinen, Elina Kalenius, Raisa Neitola, Francesco Sansone, Laura Baldini, Rocco Ungaro, Alessandro Casnati,

Pirjo Vainiotalo

Figure ESI1.  $^1\text{H}$  NMR ( $\text{CDCl}_3$ , 300 MHz, 298 K) of **6**.

Figure ESI2.  $^1\text{H}$  NMR ( $\text{DMSO-}d_6$ , 300 MHz, 363 K) of **6**.

Figure ESI3. VT-NMR spectra of **1** in  $\text{CD}_3\text{OD}$ .

Figure ESI4. a) VT-NMR spectra of **1** in  $\text{D}_2\text{O}$ , b)  $^{13}\text{C}$  NMR spectrum of **1** in  $\text{D}_2\text{O}$  298K and c) exact mass measurement and comparison of isotopic distribution for **1**

Figure ESI5. Profile spectra measured from samples containing **1** in the presence of a) Asp b) Leu  
c) Ser d) Tyr and e) Trp.

Figure ESI6. Profile spectra measured from samples containing **2** in the presence of a) Asp b) Leu  
c) Ser d) Tyr and e) Trp.

Figure ESI7. Profile spectra measured from samples containing **3** in the presence of a) Ser b) Leu c)  
Phe d) Tyr and e) Trp.

Figure ESI8. Competitive complexation of amino acids in the presence of a) **1** and b) **3**.

Figure ESI9. Molecular modelling of tetraglucocalixarene **1** carried out using *semi-empirical* methods at PM3 level: the more stable *cone* conformer a) is 123 kJ/mol more stable than the *partial cone* conformer b).

Figure ESI10. Examples of isolation and CID spectra for a)  $[\mathbf{2}+\text{Tyr-H}]^-$  and b)  $[\mathbf{3}+\text{Tyr-2H}]^{2-}$ .

Figure ESI11. Optimized structure of **3** (lateral and apical views, possible H-bonds marked with green dotted lines).

Figure ESI12. Optimized structures (density functional BP86) for a) **2**, b) **2** with Phe, c) **2** with Tyr and d) **2** with Trp (lateral and apical views, possible H-bonds marked with green dotted lines).

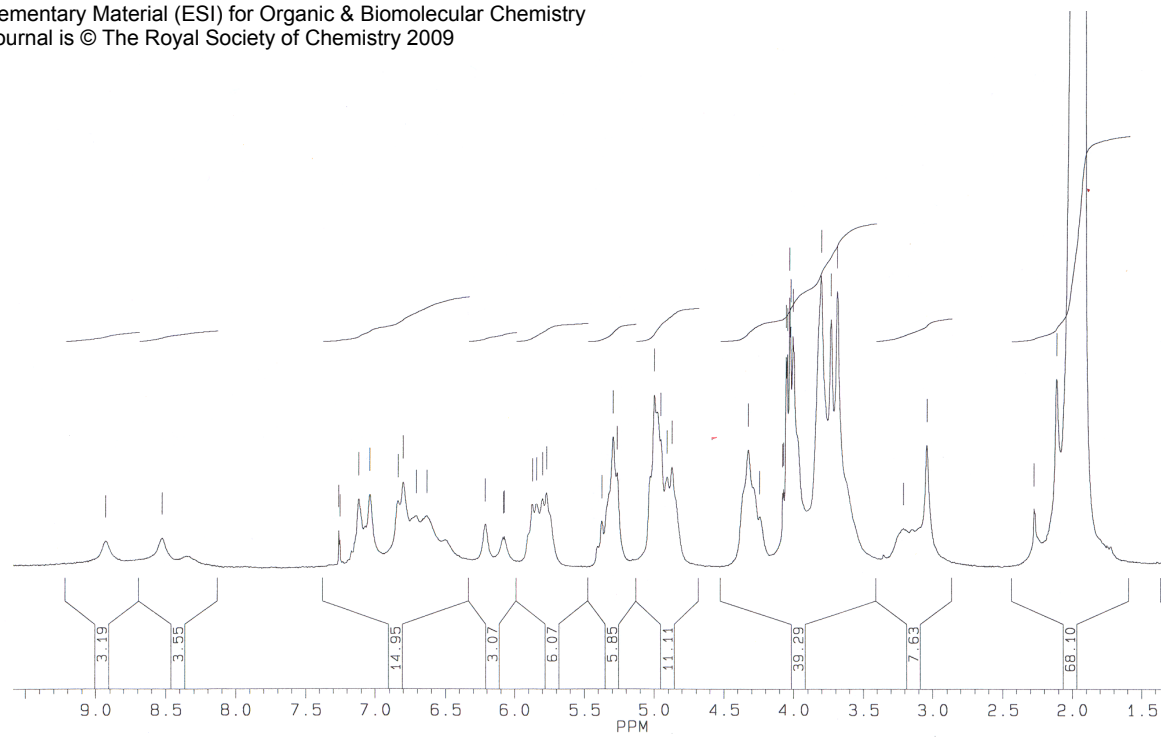


Figure ESI1. <sup>1</sup>H NMR ( $\text{CDCl}_3$ , 300 MHz, 298 K) of **6**.

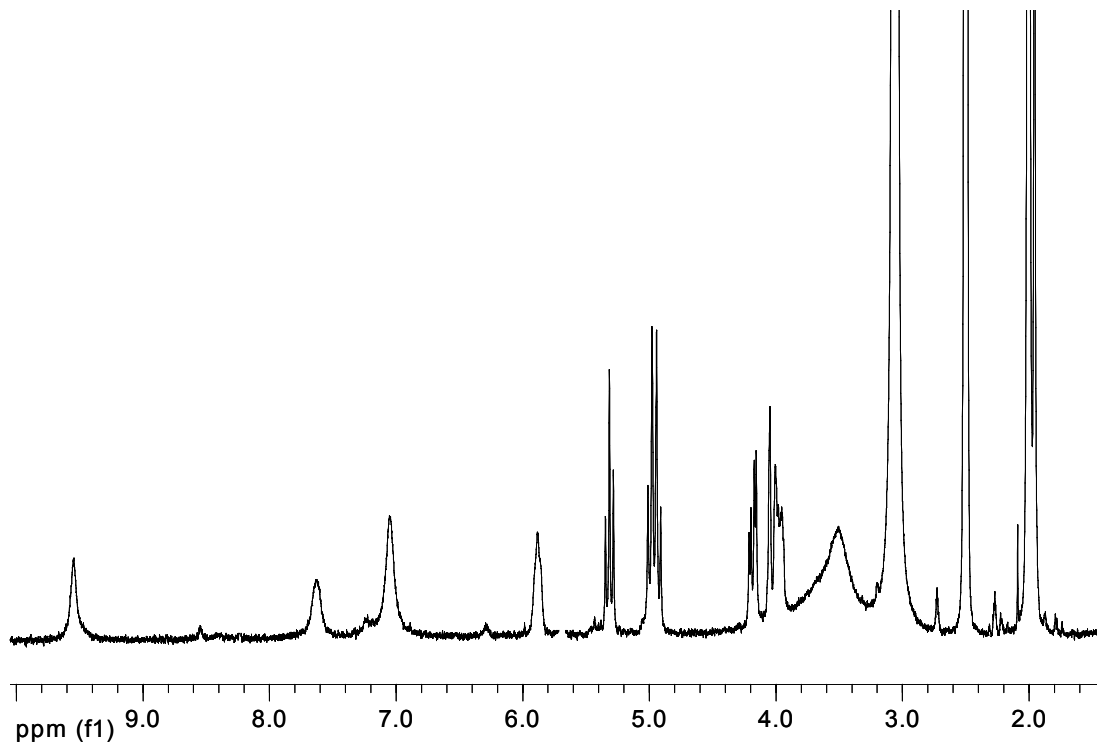


Figure ESI2. <sup>1</sup>H NMR ( $\text{DMSO}-d_6$ , 300 MHz, 363 K) of **6**.

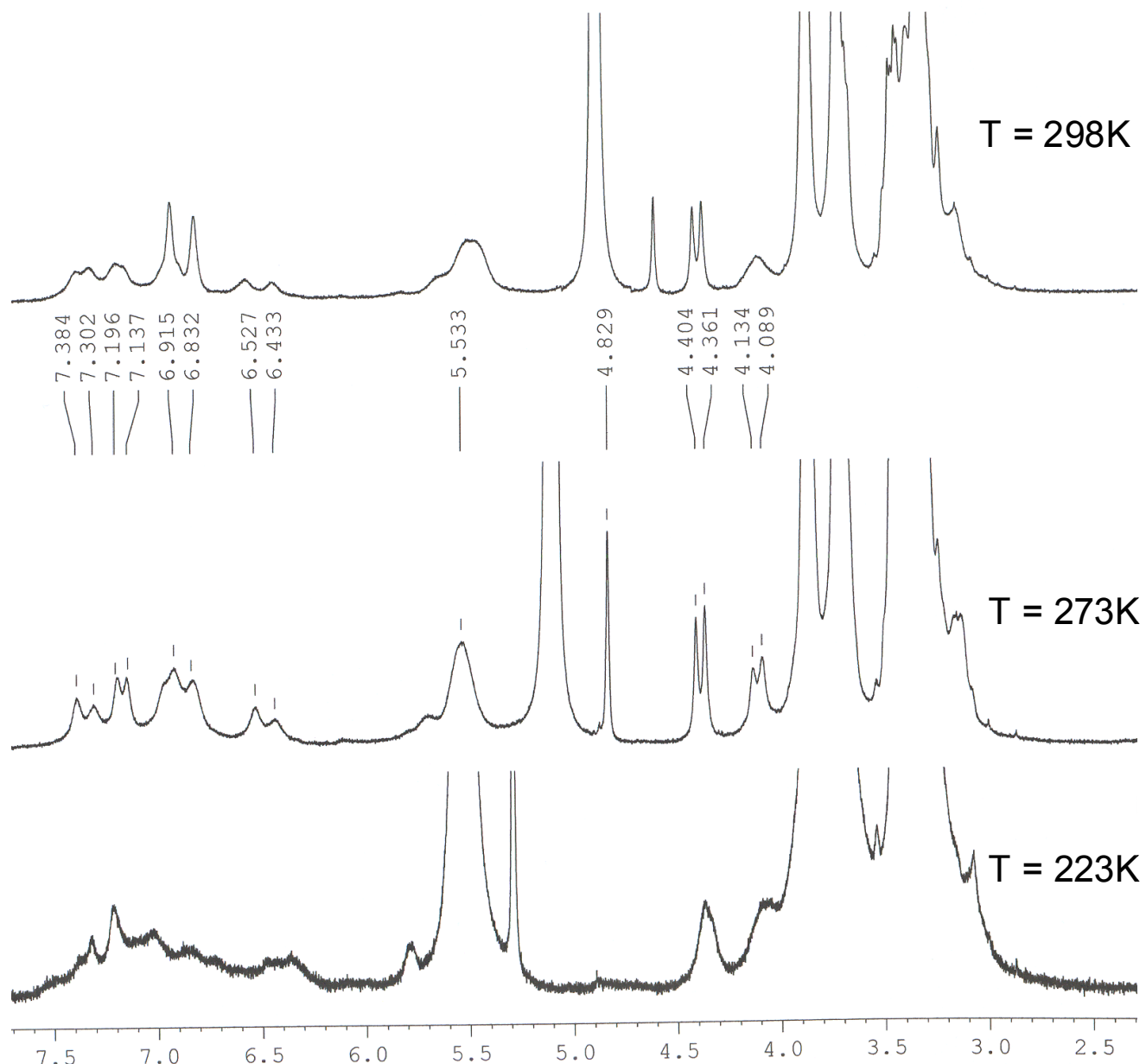
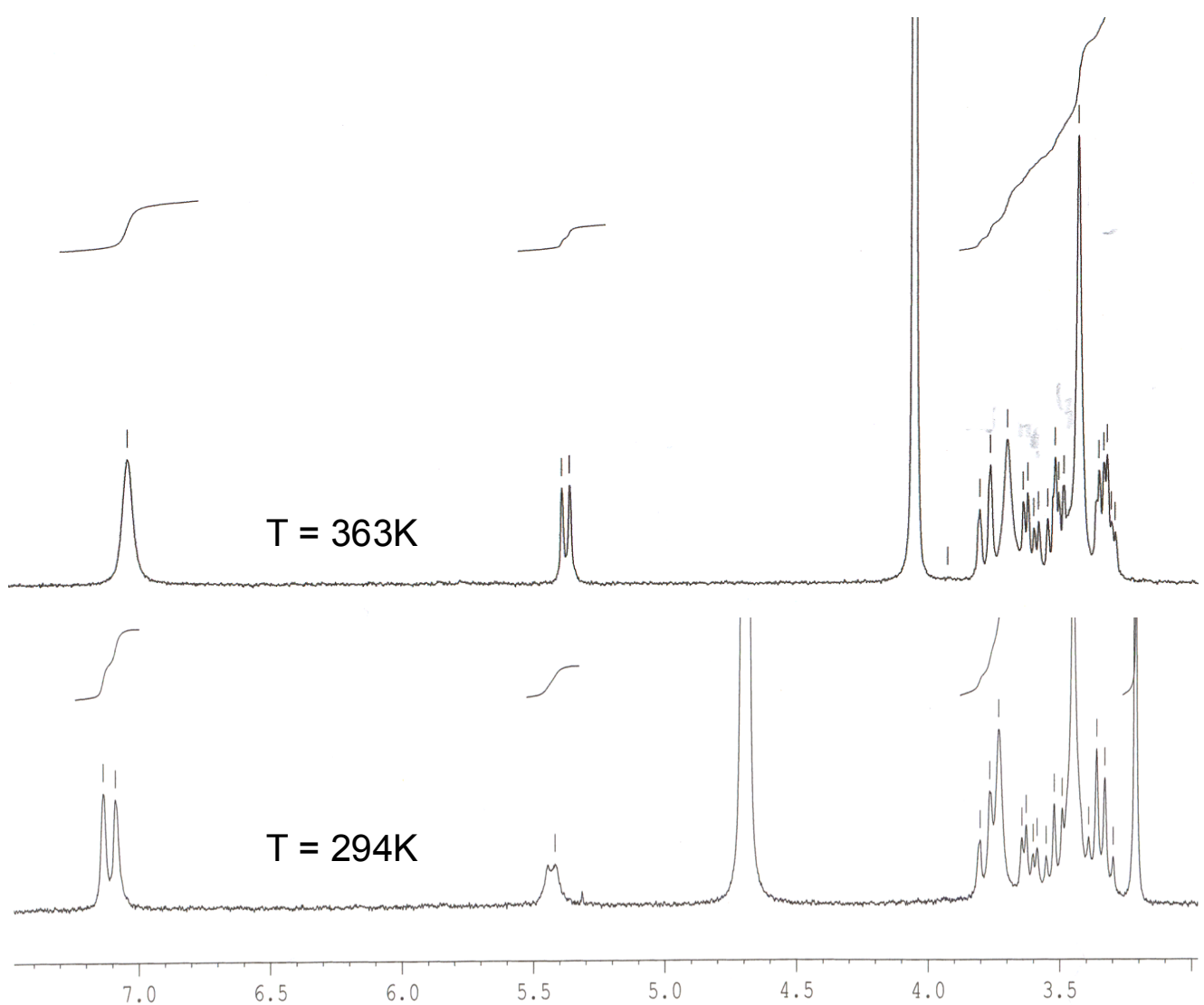
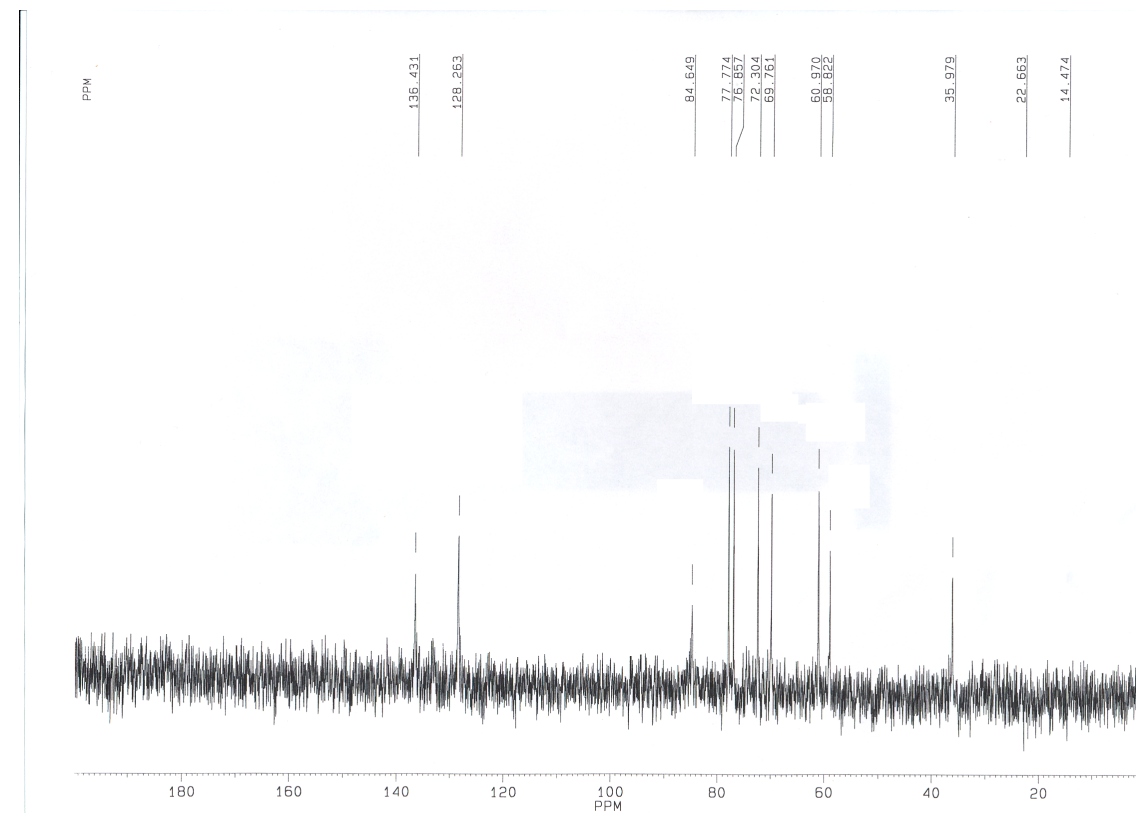


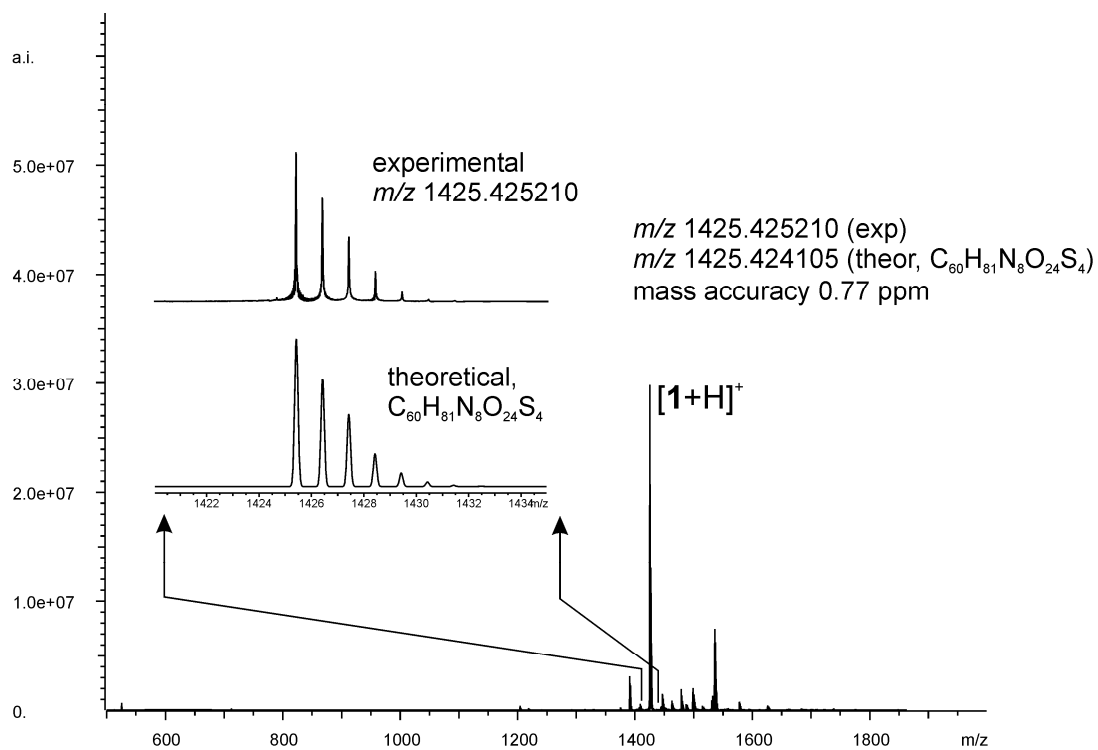
Figure ESI3. VT-NMR spectra of **1** in  $\text{CD}_3\text{OD}$ .



a)



b)



c)

Figure ESI4. a) VT-NMR spectra of **1** in  $\text{D}_2\text{O}$ , b)  $^{13}\text{C}$  NMR spectrum of **1** in  $\text{D}_2\text{O}$  298K and c) exact mass measurement and comparison of isotopic distribution for **1**

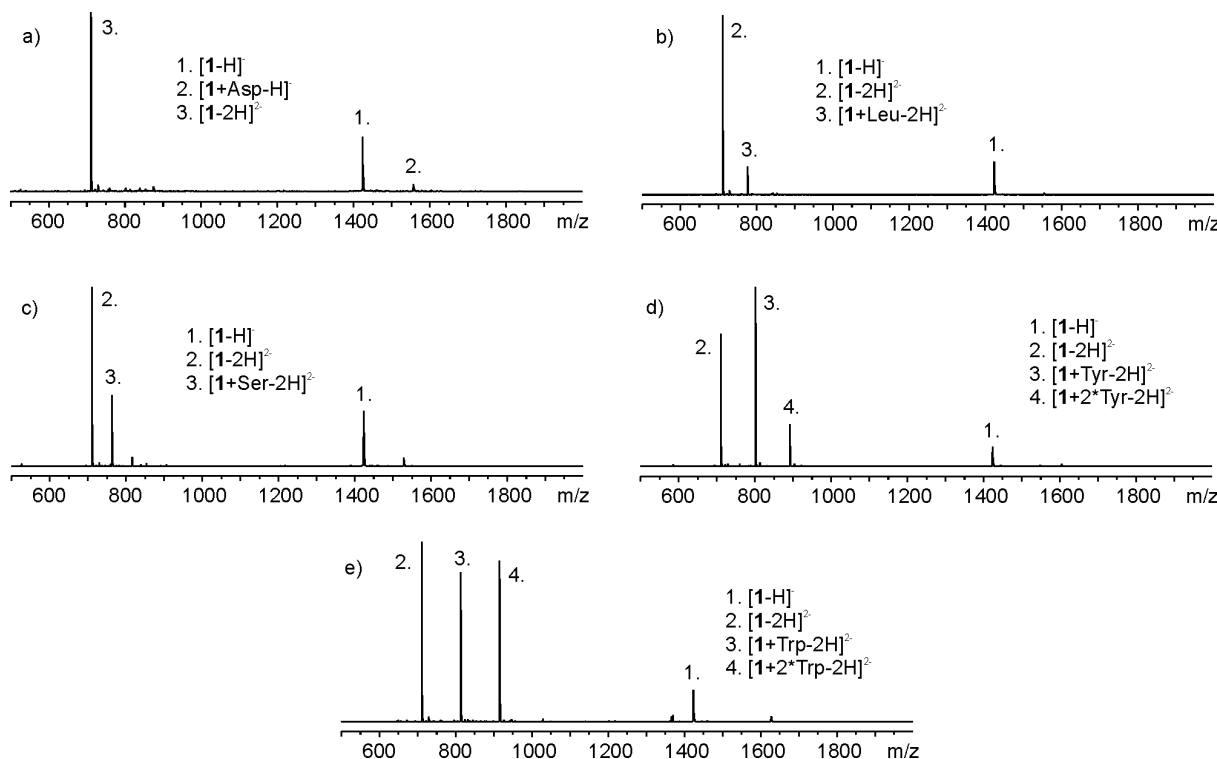


Figure ESI5. Profile spectra measured from samples containing **1** in the presence of a) Asp b) Leu c) Ser d) Tyr and e) Trp.

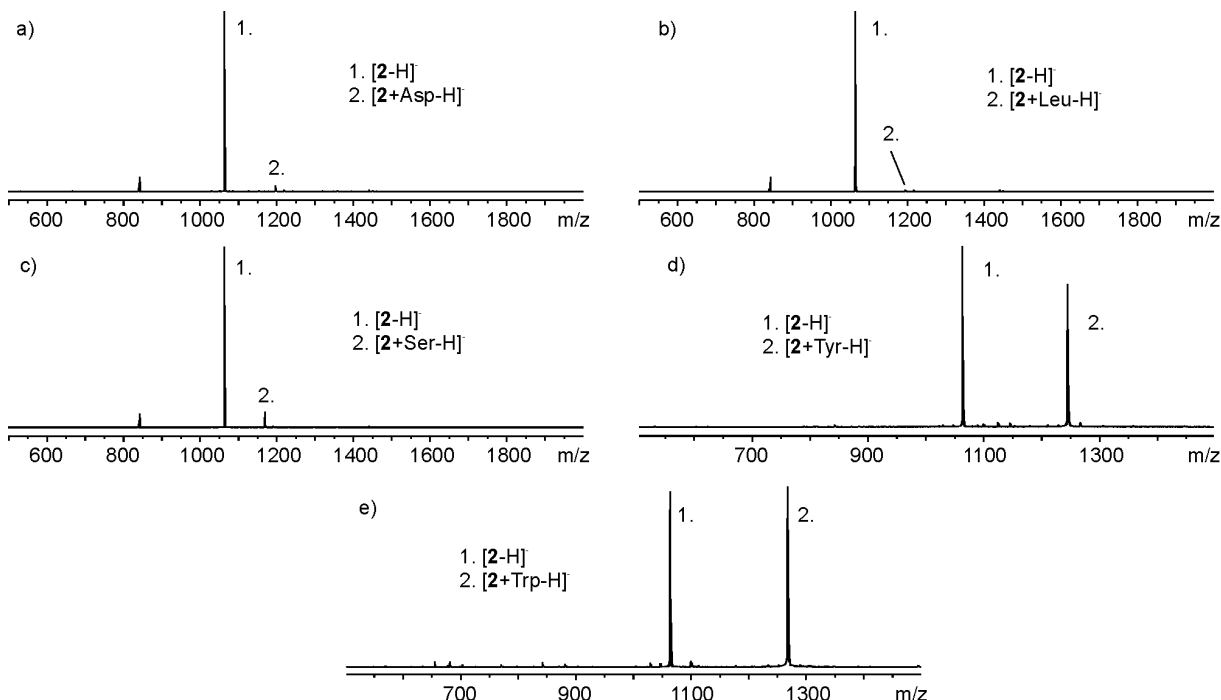


Figure ESI6. Profile spectra measured from samples containing **2** in the presence of a) Asp b) Leu c) Ser d) Tyr and e) Trp.

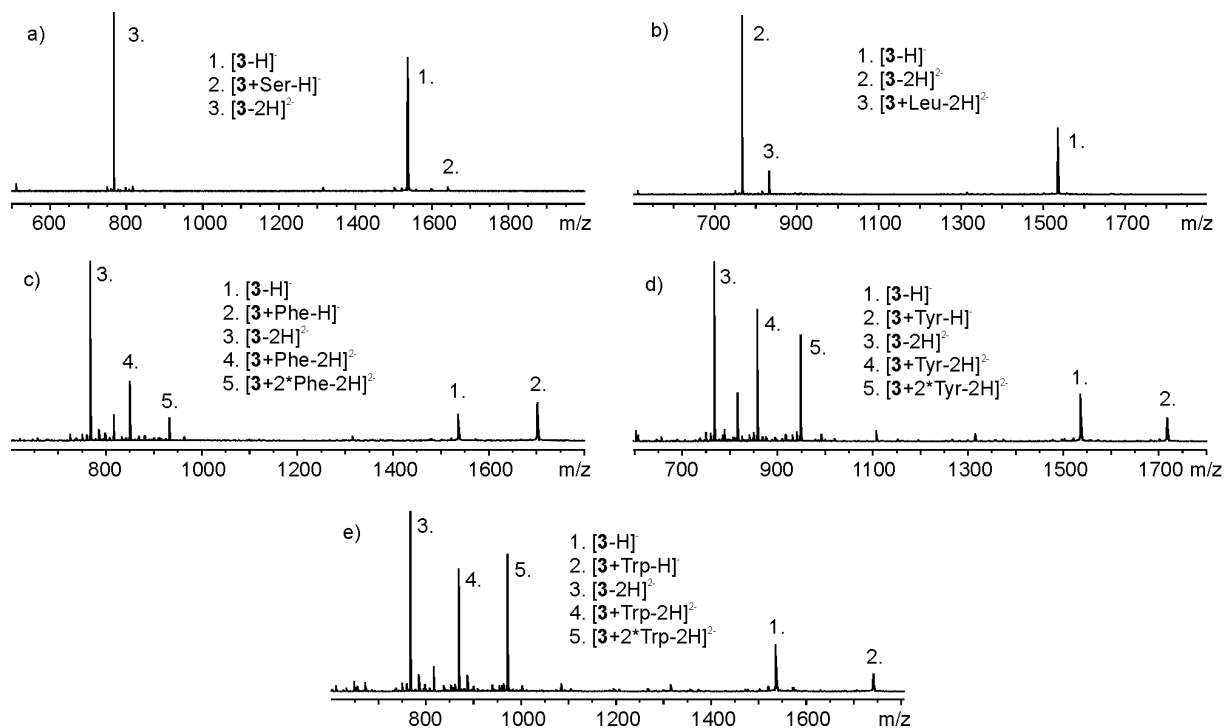


Figure ESI7. Profile spectra measured from samples containing **3** in the presence of a) Ser b) Leu c) Phe d) Tyr and e) Trp.

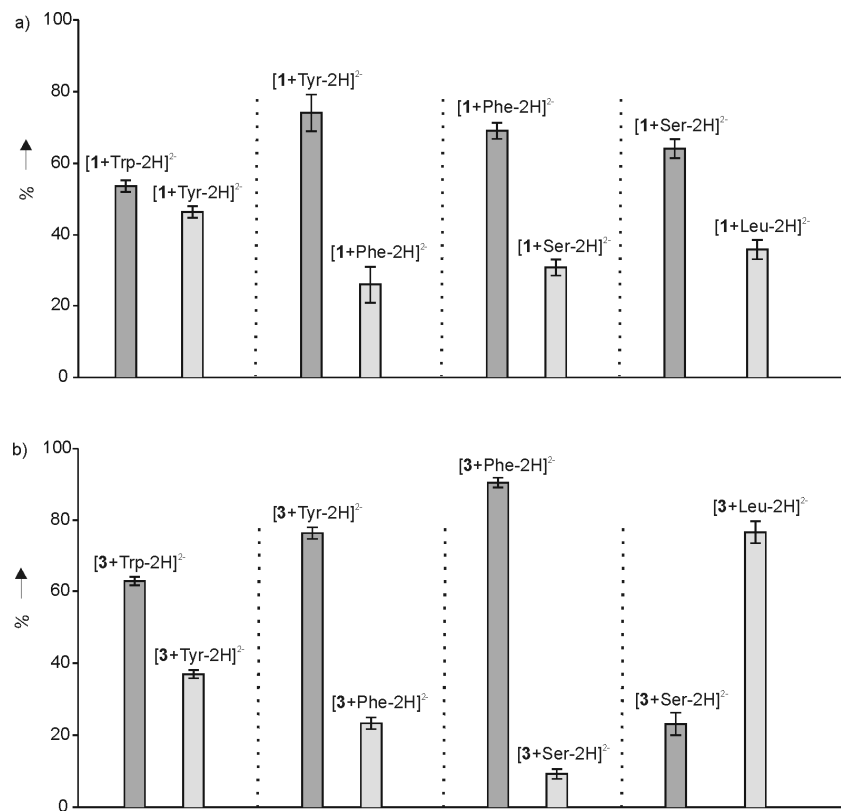
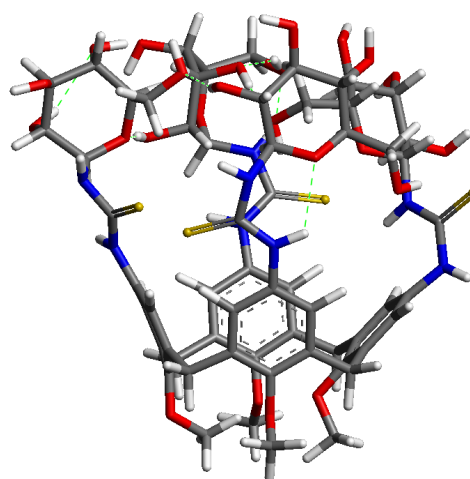


Figure ESI8. Competitive complexation of amino acids in the presence of a) **1** and b) **3**.

a)



b)

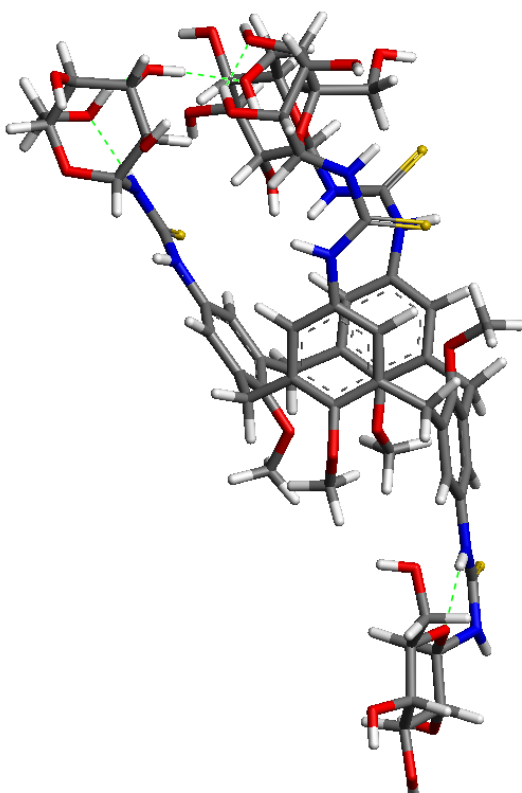


Figure ESI9. Molecular modelling of tetraglucocalixarene **1** carried out using *semi-empirical* methods at PM3 level: the more stable *cone* conformer a) is 123 kJ/mol more stable than the *partial cone* conformer b).

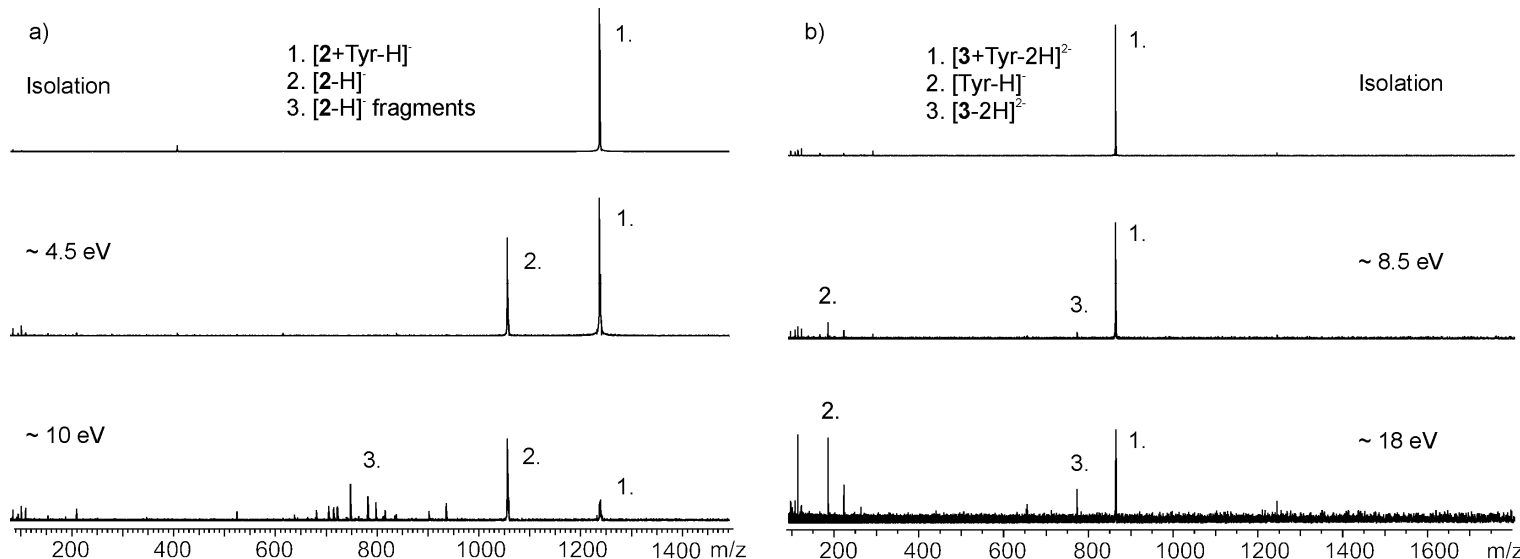


Figure ESI10. Examples of isolation and CID spectra for a)  $[2+\text{Tyr}-\text{H}]^-$  and b)  $[3+\text{Tyr}-2\text{H}]^{2-}$ .

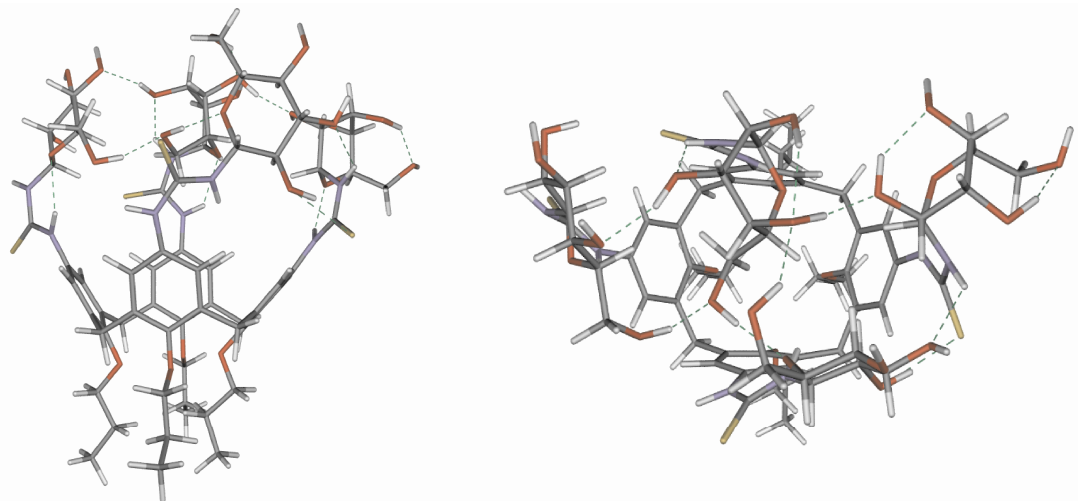


Figure ESI11. Optimized structure of **3** (lateral and apical views, possible H-bonds marked with green dotted lines).

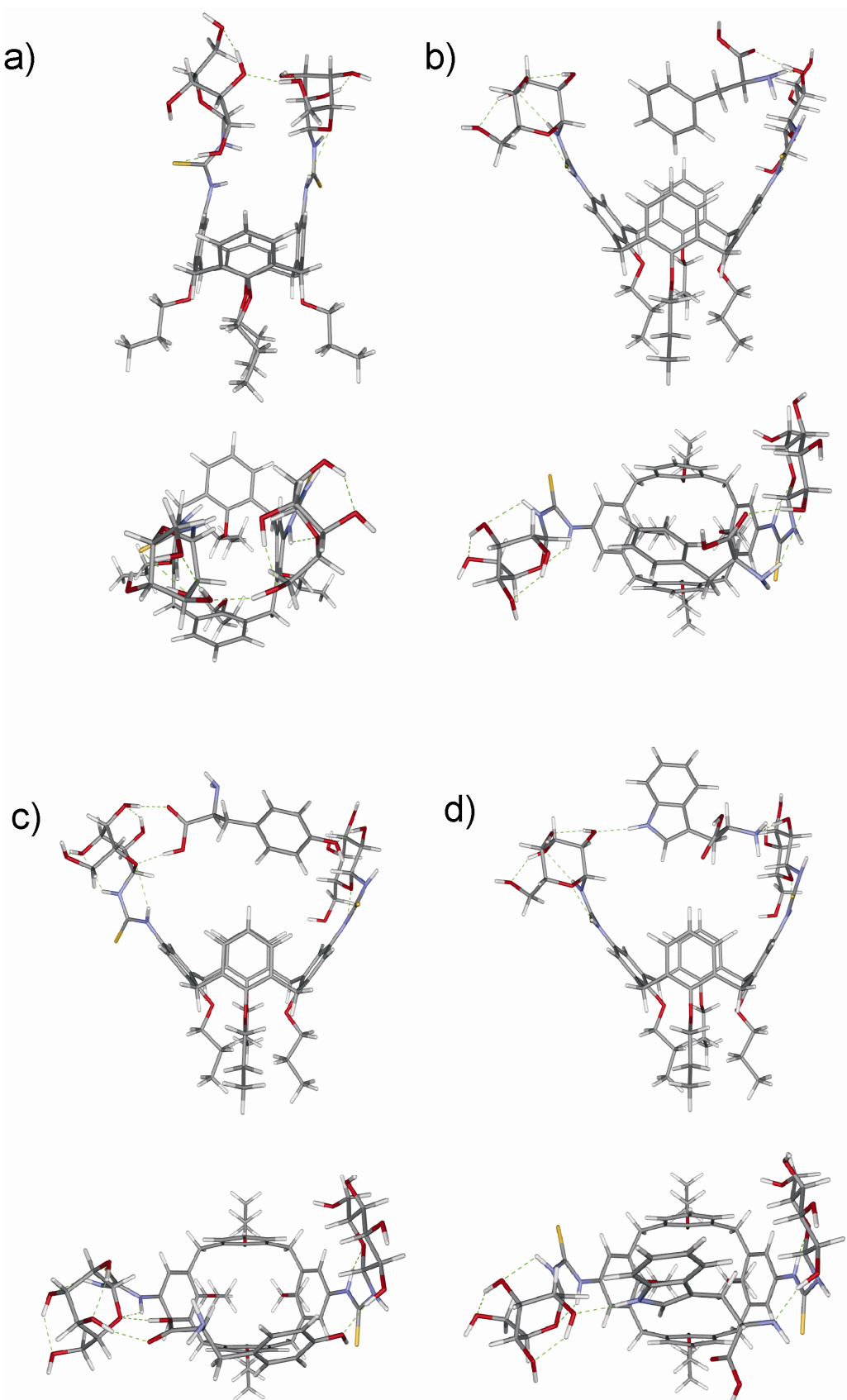


Figure ESI12. Optimized structures (density functional BP86) for a) **2**, b) **2** with Phe, c) **2** with Tyr and d) **2** with Trp (lateral and apical views, possible H-bonds marked with green dotted lines).